

Article

Main Drivers of Fecundity Variability of Mussels along a Latitudinal Gradient: Lessons to Apply for Future Climate Change Scenarios

Gabriela F. Oliveira ^{1,*} , Hanifah Siregar ², Henrique Queiroga ¹  and Laura G. Peteiro ^{3,*} 

¹ CESAM—Centre for Environmental and Marine Studies, Department of Biology, University of Aveiro, 3810-193 Aveiro, Portugal; henrique.queiroga@ua.pt

² Wildlife Conservation Society, Bogor 16128, Indonesia; hanifah.siregar@gmail.com

³ Instituto de Investigaciones Marinas (IIM), Consejo Superior de Investigaciones Científicas (CSIC), 36208 Vigo, Spain

* Correspondence: gabriela.oliveira@gmail.com (G.F.O.); lpeteiro@iim.csic.es (L.G.P.)

Abstract: Bivalve relevance for ecosystem functioning and human food security emphasize the importance of predictions of mussel performance under different climate stressors. Here, we address the effect of a latitudinal gradient of temperature and food availability on the fecundity of the Mediterranean mussel to try to better parameterize environmental forcing over reproductive output. We show that temperature plays a major role, acting as a switching on–off mechanism for gametogenesis, while food availability has a lower influence but also modulates the number of gametes produced. Temperature and food availability also show different effects over fecundity depending on the temporal scale evaluated. Our results support the view that the gametogenesis responds non-linearly with temperature and chlorophyll concentration, an issue that is largely overlooked in growth, production and energy budgets of bivalve populations, leading to predictive models that can overestimate the capability of the mussel’s populations to deal with climate change future scenarios.

Keywords: reproductive output; latitudinal gradients; temperature; food availability; *Mytilus galloprovincialis*; climate change; bivalves



Citation: Oliveira, G.F.; Siregar, H.; Queiroga, H.; Peteiro, L.G. Main Drivers of Fecundity Variability of Mussels along a Latitudinal Gradient: Lessons to Apply for Future Climate Change Scenarios. *J. Mar. Sci. Eng.* **2021**, *9*, 759. <https://doi.org/10.3390/jmse9070759>

Academic Editor:
Dariusz Kucharczyk

Received: 16 June 2021
Accepted: 5 July 2021
Published: 9 July 2021

Publisher’s Note: MDPI stays neutral with regard to jurisdictional claims in published maps and institutional affiliations.



Copyright: © 2021 by the authors. Licensee MDPI, Basel, Switzerland. This article is an open access article distributed under the terms and conditions of the Creative Commons Attribution (CC BY) license (<https://creativecommons.org/licenses/by/4.0/>).

1. Introduction

The accumulation of evidence on climate change impact on marine ecosystems increasingly points towards complex cascading effects at different levels of biological organization [1–5]. Rising atmospheric CO₂ has consequences not only for ocean temperature and acidification, but also on circulation patterns, stratification, or oxygen content [3,4]. Physical and chemical changes derived from anthropogenic activity have direct and indirect effects on physiology, behaviour and interactions of marine organisms, with consequences at population and community levels, compromising ecosystem functioning and finally its ability to provide a range of goods and services to humans [2–5].

Understanding and foreseeing the response of marine populations to climate change is crucial for human planning and development of mitigation and adaptation measures [3,6,7]. A commonly employed approach is to couple population and climate models to test for the effect of different climate scenarios on species distribution, performance or productivity [3,7–9]. Many of these studies agree to identify reef forming calcified organisms (corals, mussels, oysters, etc.) as one of the most vulnerable, because of their particular sensitivity to ocean acidification and other cascading effects related to the rising temperatures [1,3,10].

Mussels are amongst the most studied reef forming organisms, not just because of their interest as ecological engineers, driving biodiversity patterns [11] or regulating benthic-pelagic coupling process and water quality [12,13], but also because of their relevance for aquaculture and food security [14]. Recommendations of scientific advisory committees

for a sustainable response to the increasing human demand of animal protein include an increment of bivalve production by 100 Mt before 2030 [15]. The large vulnerability of bivalves coupled to their relevance for food security emphasizes the importance of accurate predictions of mussel performance under different climate change scenarios, and has prompted the use of this species as a model for the study of the impact of several stressors [16–19].

Reproductive success is a key process controlling population dynamics, and identifying the environmental drivers that control reproductive output is key to be able to forecast the consequences of climate change [7,20,21]. The reproductive cycle of bivalves and other invertebrates comprises a sequence of biological events comprising gametogenesis, spawning and a resting period before gonad restoration [22]. This cycle is controlled by endogenous and environmental factors, and their interactions influence the onset and the duration of the reproductive cycle [22]. Among these environmental factors, temperature and food availability are considered to be the main factors regulating reproduction in marine invertebrates [20–24]. Temperature is usually regarded as a trigger for spawning, but also regulates the rate of gonadal development with a cumulative effect [20–24]. Food availability has been directly associated to fecundity (number of gametes produced) [24,25] although some authors also pointed to phytoplankton blooms as a spawning cue, which allows matching larval development with optimal environmental conditions [26].

Under unfavourable environmental conditions, bivalves activate costly defence and repair mechanisms, which reallocate energy away from reproduction towards somatic maintenance [16,20]. Therefore, reabsorption of gametes and fecundity loss are expected consequences of stressing scenarios which will become more persistent in the future [1,3]. Nonetheless, studies forecasting reproductive output and performance of bivalve populations, based on the Dynamic Energy Budget (DEB) principle, consistently predict a maintenance or a slight increase of reproductive output for bivalves in all the locations where warming future scenarios don't overpass thermal tolerance of the species [7,9,20,23,27–30].

DEB and other models assume that physiological rates are proportional to size and follow at least a temperature-dependent relationship according to the optimal physiological range for somatic maintenance of the species, but do not usually consider specific environmental limits for gamete development [31–33]. Even when many attempts have been made to increase the complexity of the description of energy allocation to reproduction to make it more realistic [23], specific non-linear responses of gamete production to environmental conditions are not taken into account. Optimum values of temperature and food availability might differ between somatic and gametogenic processes. For example, while temperature tolerance ranges of *Mytilus galloprovincialis* range from 5 °C to 35 °C, with an optimum for somatic maintenance around 17.5 °C [28], some studies have determined a reproduction limiting temperature of 19 °C for the same species, with an optimum for the production of vitellogenic oocytes around 14 °C [34].

A correct parameterization of the complex relationships between environmental drivers and gamete production requires a better understanding of the underlying processes. Knowledge about the scales of spatial and temporal variability in reproductive output coupled to environmental variability is essential to gain a better understanding of the reproductive physiology, and to be able to incorporate it properly in the prediction of future scenarios.

In this study, we examined the variability in reproductive outputs of a series of populations of *Mytilus galloprovincialis* along a latitudinal gradient covering the Portuguese coast during the main reproductive season (Spring) for two different years. Consistency of latitudinal patterns of fecundity between years along with environmental variability was explored to identify relationships along an environmental gradient. Our goal was to identify non-linear relationships between gamete production and environmental variables at different temporal scales, to understand their influence when looking at the complete gametogenesis process (≈ 4 months) or to the last phases of gamete maturation. That

information might help to provide a better parameterization of reproduction, and to develop more accurate models for mussel populations forecasting.

2. Materials and Methods

2.1. Sampling Design

Mediterranean mussels, *Mytilus galloprovincialis*, were collected at 7 sites along the Portuguese coastline in 2014 and 2017 (Figure 1) following a latitudinal gradient from North to South: Póvoa do Varzim, Costa Nova, Peniche, Cascais, Galapos and Zavial. Sampling locations ranged from around 37° N to 41° N (distance \approx 560 km, mesoscale), and took place during spring in 2014 and 2017 (14 April to 4 May 2014 and 18 May to 22 June 2017). At each site, 150 individuals were collected randomly along the intertidal, for length frequency and fecundity analysis.

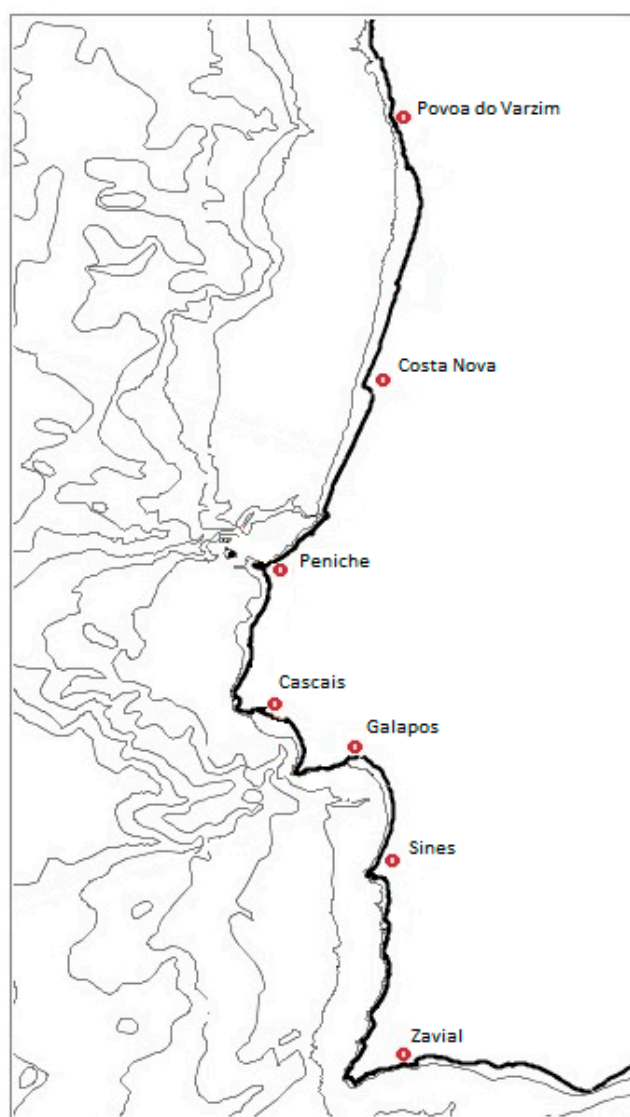


Figure 1. Fecundity sampling locations along the Portuguese coastline.

2.2. Environmental Variables

Sea Surface Temperature (SST), Sea Surface Salinity (SSS) and Chlorophyll-a concentration (Chl-a) as environmental variables were obtained from the beginning of the year to the sampling date at each location. Daily averaged values of SST ($^{\circ}$ C) and SSS of 2014 were provided by Hycom model (<http://www.hycom.org>) and values of Chl-a concentration (mg/m^3) were obtained from interpolation of satellite data (MODIS, SeaWiFS and

MERIS) supplied by CERSAT/IFREMER (<http://ftp.ifremer.fr/ifremer/cersat/products/gridded/ocean-color/atlantic/EURL4-CHL-ATL-v01>) (both accessed on 4 July 2014). The SST and SSS values of 2017 were obtained from the Mercator Ocean (Daily Global Analysis and Forecast of Ocean Physics, <http://www.mercator-ocean.fr>, EU Copernicus Marine Environment Monitoring Service, accessed on 7 November 2017), resolution 1/12° (≈7 km for medium latitudes). Values of Chl-a concentration (mg/m³) were obtained from CMEMS Products (Copernicus-GlobColour Project, ACRI-ST, EU Copernicus Marine Environment Monitoring Service, accessed on 7 November 2017), which consist of daily data interpolated and reprocessed (multi-year time series) from satellite observations (SeaWiFS, MODIS-Aqua, MERIS and VIIRS), and have a horizontal resolution of 1 km. Based on these data, a set of variables regarding temperature and food availability were created to identify different effects of environmental variability, at long and short-time scales, on fecundity. Concerning short-term effects, monthly averaged SST (average SST, °C) and Chl-a concentration (average Chl-a, mg/m³) during the month preceding the sampling date were calculated for each location. Data from 2014 for Cascais, Sines and Zavial were unavailable, so these were not included in the analysis. Looking at the long-term effects, we calculated the averaged Chl-a concentration during 10 days around the peak of the spring transition (Max Chl-a) and the number of days with SST over 14 °C (T > 14 °C) during the 4 months previous to the sampling date for each location to match the expected gametogenesis duration [35,36]. The threshold of 14 °C was selected based on the temperature optimum reported in laboratory experiments for the production of vitellogenic oocytes [34].

2.3. Fecundity Analysis

All mussels collected were measured along their anterior–posterior axis to calculate their total length (L, mm), using a digital calliper. Samples were divided into size classes with 10 mm intervals, from 5 mm to 95 mm (no individuals larger than 100 mm were detected in the intertidal). From each size class, 5 females were randomly selected for fecundity analysis. Females were first identified visually based on the orange coloration of their gonads and the presence of oocytes confirmed under a stereomicroscope. From the gonads of each female, a 1 cm diameter sample was taken to assess fertility, according to the methodology presented in Sukhotin and Flyachinskaya [37]. Each gonad sample was weighed, gently macerated and diluted with 20–25 mL of salted water. From this dilution, 3 sub-samples between 150–250 µL were taken to count the oocytes under a microscope, with the help of a Bogorov counting chamber. Another gonad sample (1 cm) was taken to estimate the weight of the tissue used for oocytes quantification. The rest of the gonad was separated from the remaining soft tissues to estimate the weight of gonads with regard to the rest of tissues. After dissecting, all samples were dried at 60 °C for 24 h to obtain dry weights.

Absolute fecundity (AF, number of oocytes/female) and relative fecundity (RF, number of oocytes/g gonad) were estimated according to the following formulas:

$$AF = \bar{N} \left(\frac{W_g V_d 100}{W_s V_s 95} \right) \quad RF = \frac{AF}{W_g}$$

where \bar{N} is the average number of oocytes observed in 3 subsamples, W_g is the dry weight of the total gonad (g), W_s is the dry weight of the gonad sample extracted for the oocyte count (g), V_d is the volume of water where the oocytes were diluted (mL), and V_s is the volume used in the subsamples for counting oocytes (mL). Since the extraction of oocytes from the samples is only 95% efficient, with 5% of oocytes remaining in the tissues during the extraction process [37], a 100/95 correction factor was applied to the estimate of AF.

2.4. Statistical Analysis

In order to evaluate the temporal and spatial variability of the AF and RF we used factorial ANOVAs with location and year as fixed factors. The relationship between size

and AF was analysed with ANCOVA (Separate Slopes model), separately for each year, including size (L , mm) as a covariable and location (Loc, 7 levels) as a fixed factor. In these analysis AF, RF and Size were log-transformed. The data and residues were evaluated for normality (Q-Q plot and Shapiro-Wilk Normality Test) and homoscedasticity (Levene's Test). ANOVAs and ANCOVAs were performed using the software Statistica 12 (Stat Soft, Tulsa, OK, USA).

Generalized additive models (GAM), as implemented in the mgcv library of R 3.6.2 [38], were used to investigate the seasonal patterns (day of the year) and local variation (location) of the environmental variables measured (SST, SSS and Chl-a). GAM models were also employed to investigate the relationships between the environmental parameters (days > 14.5, average SST, average SSS, max Chl-a) on RF (log-transformed). The Akaike information criterion (AIC) was used to select the optimal set of variables for inclusion in the model. Model validation included the verification of homogeneity, normality and independence assumptions [39].

3. Results

3.1. Environmental Variables

Seasonality largely explained the variability observed in temperature and salinity (77.7 to 86.5% of deviance explained by the variables location and day of the year; Table 1, Figure 2). Latitudinal patterns were consistent during both sampling years, with a temperature and salinity increase from North to South (Table 1). Nonetheless, the estimated coefficients revealed warmer temperatures and lower salinities in 2017 (Table 1).

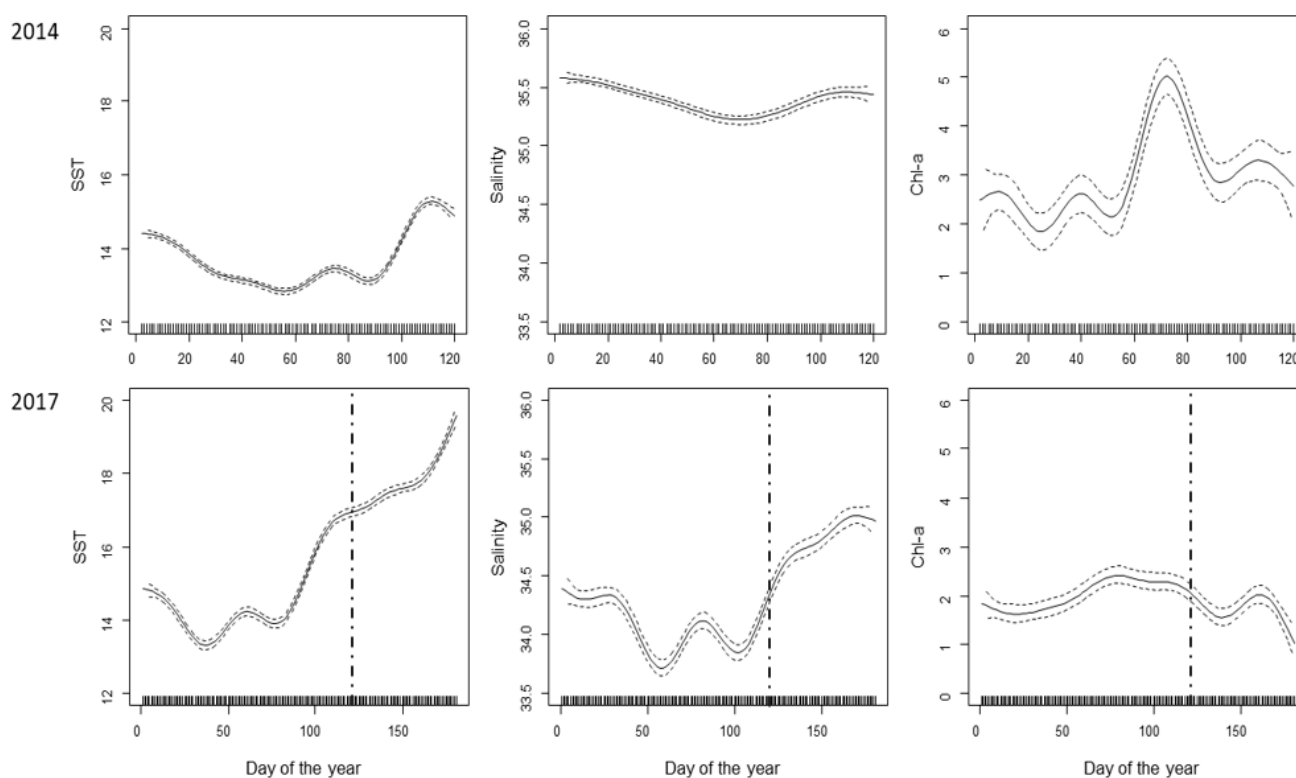


Figure 2. Estimated smoothing curves of day of the year for Sea Surface Temperature (SST, °C), Sea Surface Salinity (SSS) and Chlorophyll-a concentration (Chl-a, mg/m³) from 2014 and 2017, expressed as a mean between locations along the Portuguese coastline. Results of the General Additive Model showing the effect of the variable “day of the year” (Julian year). Dashed lines show a 95% Confidence Interval and tick marks along the x-axis represent when observations occurred. Vertical dashed line (2017) is a reference to the last day from 2014 (day 120).

Table 1. Structure of the General Additive Model describing Sea Surface Temperature (°C), Sea Surface Salinity (SSS) and Chlorophyll-a concentration (mg/m³) variability along the coastline from January to May 2014 and January to June 2017. S.E.: standard error; e.d.f.: estimated degrees of freedom.

		SST (°C)				SSS				Chl-a (mg/m ³)			
2014		Parametric Coefficients				Parametric Coefficients				Parametric Coefficients			
Location	Estimate	S.E.	t	p	Estimate	S.E.	t	p	Estimate	S.E.	t	p	
Póvoa do Varzim (Intercept)	13.357	0.031	436.581	p < 0.001	35.294	0.017	2051.909	p < 0.001	2.499	0.138	21.488	p < 0.001	
Costa Nova	0.287	0.044	−6.541	p < 0.001	0.103	0.024	−4.239	p < 0.001	0.476	0.196	−6.427	p < 0.050	
Peniche	0.486	0.044	11.077	p < 0.001	0.611	0.024	25.197	p < 0.001	−1.258	0.196	−6.427	p < 0.001	
Cascais	0.667	0.052	12.883	p < 0.001	0.418	0.029	14.651	p < 0.001	-	-	-	-	
Galapos	0.730	0.044	16.614	p < 0.001	0.512	0.024	21.103	p < 0.001	−0.698	0.196	−3.563	p < 0.001	
Sines	1.103	0.052	21.310	p < 0.001	0.611	0.029	24.423	p < 0.001	-	-	-	-	
Zavial	1.571	0.062	25.430	p < 0.001	0.746	0.034	21.903	p < 0.001	-	-	-	-	
		Smooth terms (non parametric)				Smooth terms (non parametric)				Smooth terms (non parametric)			
		e.d.f	F	p	e.d.f	F	p	e.d.f	F	p			
Day of the Year	8.94	302.6	p < 0.001		6.07	34.04	p < 0.001		8.61	16.3	p < 0.001		
		R ² adjusted: 0.861		% Deviance explained: 86.5%	R ² adjusted: 0.772		% Deviance explained: 77.7%	R ² adjusted: 0.278		% Deviance explained: 29.6%			
2017		Parametric coefficients				Parametric coefficients				Parametric coefficients			
Location	Estimate	S.E.	t	p	Estimate	S.E.	t	p	Estimate	S.E.	t	p	
Póvoa do Varzim (Intercept)	15.051	0.057	276.091	p < 0.001	33.215	0.032	1059.370	p < 0.001	1.718	0.080	24.265	p < 0.001	
Costa Nova	0.623	0.080	−7.757	p < 0.001	1.112	0.046	−24.270	p < 0.001	0.224	0.113	−0.198	0.843	
Peniche	0.174	0.080	2.168	p < 0.050	0.667	0.046	14.550	p < 0.001	−0.496	0.113	−4.384	p < 0.001	
Cascais	0.569	0.080	7.084	p < 0.001	0.940	0.046	20.520	p < 0.001	−0.180	0.113	−1.593	0.111	
Galapos	0.921	0.080	11.477	p < 0.001	1.404	0.046	30.640	p < 0.001	−0.495	0.113	−4.373	p < 0.001	
Sines	1.149	0.080	14.306	p < 0.001	1.562	0.046	34.090	p < 0.001	−1.132	0.113	−10.004	p < 0.050	
Zavial	1.489	0.080	18.544	p < 0.001	1.759	0.046	38.380	p < 0.001	−1.241	0.113	−10.970	p < 0.001	
		Smooth terms (non parametric)				Smooth terms (non parametric)				Smooth terms (non parametric)			
		e.d.f	F	p	e.d.f	F	p	e.d.f	F	p			
Day of the Year	8.94	767.6	p < 0.001		8.88	119.5	p < 0.001		8.518	12.03	p < 0.001		
		R ² adjusted: 0.862		% Deviance explained: 86.3%	R ² adjusted: 0.846		% Deviance explained: 84.8%	R ² adjusted: 0.208		% Deviance explained: 21.7%			

On the other hand, day of the year had a lower effect on the variability of Chl-a, with around 20%–30% of variance explained, much less than that observed for SSS or SST (Table 1; Figure 2). Both years maintained a similar latitudinal pattern for Chl-a, with a decreasing trend from North to South but with a maximum in Costa Nova (Table 1). Nonetheless, during 2014, the Chl-a peak related to spring transition was much more pronounced than during 2017 (Figure 2), and averaged estimated parameters also indicated larger concentrations of Chl-a during 2014 (Table 1).

3.2. Fecundity

Both indicators of fecundity, AF and RF, showed a significant interaction between location and year (Table 2). With regard to the absolute fecundity, larger values were observed in 2017 in comparison with 2014, and in spite of the significant interaction between year and location (Table 2), the latitudinal pattern was quite similar during both sampling years (Figure 3A). With the exception of Zavial, which showed an opposite trend between years, the larger number of eggs produced per individuals were consistently detected at Costa Nova Peniche and Cascais (Figure 3A). Average size of the mussel populations also showed a predominance of larger individuals at those locations (Figure 3B).

Table 2. Results of Factorial Analysis of Variance (ANOVA) of absolute fecundity (AF, log) and relative fecundity (RF, log) with locations and year as fixed factors (d.f.: estimated degrees of freedom, MS: mean squares).

AF (log)				
Effect	df	MS	F	p
Location	6	3.918	9.950	<0.001
Year	1	15.472	39.280	<0.001
Loc x Year	6	2.173	5.520	<0.001
Error	255	0.394	-	-
RF (log)				
Effect	df	MS	F	p
Location	6	1.490	8.030	<0.001
Year	1	0.108	0.580	0.446
Loc x Year	6	2.590	13.960	<0.001
Error	255	0.186	-	-

A positive linear relationship between AF and female size was observed for both sampling years, in all locations but Sines in 2014 (Tables 3 and 4). In this case, the lack of relationship between both variables might be related to the narrow range of sizes sampled (25.5–35.9 mm) in that particular location and year. Although AF maintained a positive relationship with size in every location, the significant interaction between location and size indicates differences among locations on the relevance of size on determining the amount of oocytes produced (Table 3) and therefore on the value of the fitted slopes (Figure 3C; Table 4). Nonetheless, similar slopes were fitted for each location at different years (with the exception of Sines), suggesting this relationship to be quite stable at each location (Figure 3C; Table 4).

Table 3. Results of Analysis of Covariance (ANCOVA) with Separate Slopes of Absolute Fecundity (AF, log) in different locations with size (mm, log) as covariate (d.f.: estimated degrees of freedom, SS: sum of squares, MS: mean squares).

ANCOVA with Separate Slopes: AF (log) vs. Location and Size (log)					
2014					
Effect	Df	SS	MS	F	p
Intercept	1	1.212	1.212	5.197	$p < 0.05$
Location × log size	7	17.152	2.450	10.506	$p < 0.05$
Location	6	1.590	0.265	1.137	0.346
Error	110	25.653	0.233	-	-
Total	123	59.150	-	-	-
2017					
Effect	Df	SS	MS	F	p
Intercept	1	2.343	2.343	10.624	$p < 0.05$
Location × log size	7	28.736	4.105	18.613	$p < 0.05$
Location	6	4.015	0.669	3.034	$p < 0.05$
Error	131	28.892	0.221	-	-
Total	144	81.505	-	-	-

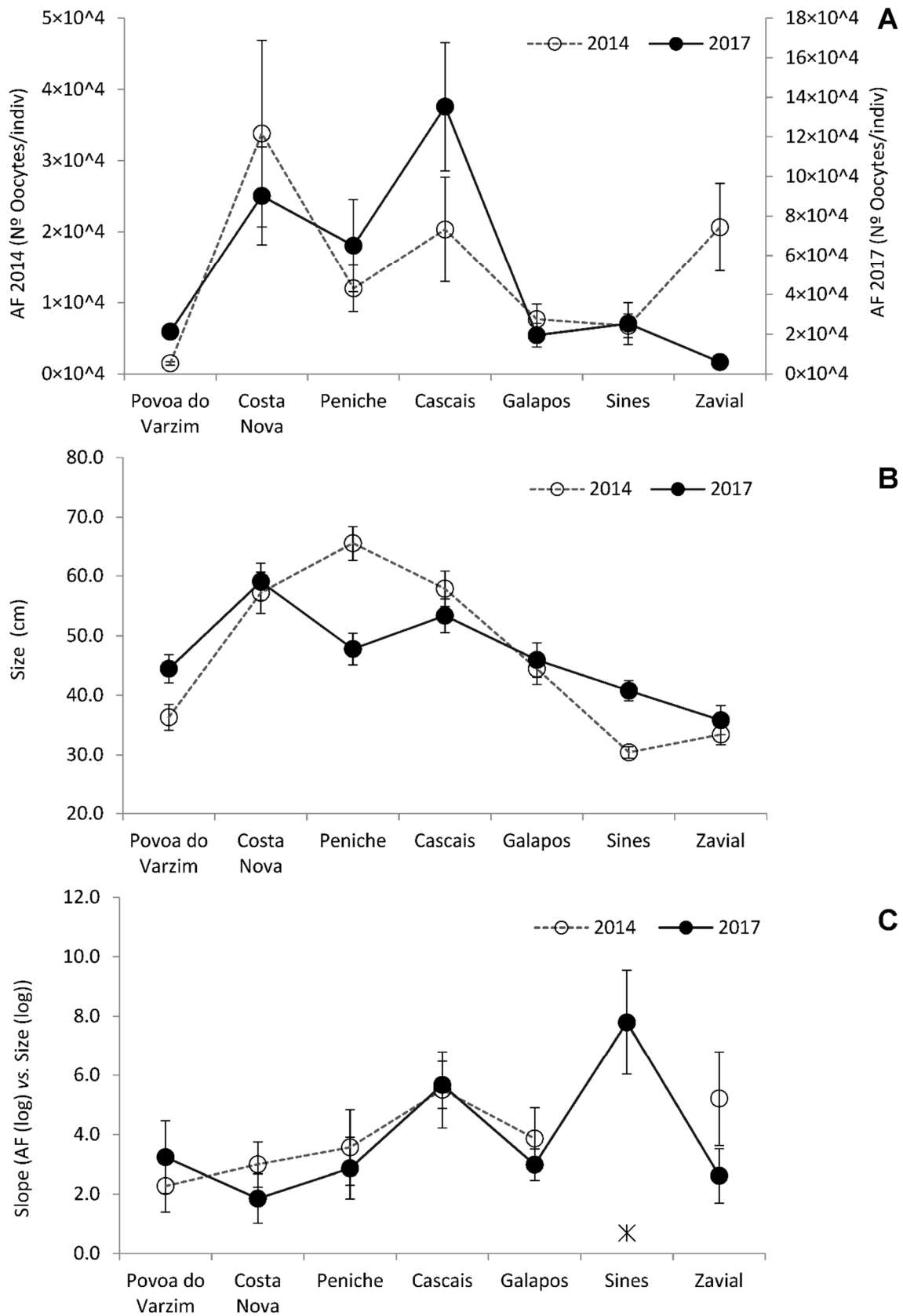


Figure 3. Average and standard error of (A) absolute fecundity (AF, n^o. oocytes per individual), (B) Size (mm) and (C) Coefficients Slopes of Analysis of Covariance (ANCOVA) between AF (logarithm-transformed) and Size (log), significant values ($p < 0.05$), except to Sines. Data of the different locations along the Portuguese coastline, from North (left) to South (right), during the years 2014 and 2017.

Table 4. Coefficients of ANCOVA with Separate Slopes analysis of absolute fecundity (AF, log) in different locations with size (mm, log) as covariate (d.f.: estimated degrees of freedom, SS: sum of squares, MS: mean squares).

Separate Slopes Coefficients: AF (log) vs. Location and Size (log)				
2014				
Location	Slope	S.E.	t	p
Povoa do Varzim	2.268	0.871	2.603	$p < 0.05$
Costa Nova	2.996	0.759	3.949	$p < 0.05$
Peniche	3.565	1.270	2.807	$p < 0.05$
Cascais	5.503	1.284	4.286	$p < 0.05$
Galapos	3.862	1.034	3.734	$p < 0.05$
Sines	0.687	2.737	0.251	0.802
Zavial	5.209	1.576	3.305	$p < 0.05$
2017				
Location	Slope	S.E.	t	p
Povoa do Varzim	3.237	1.220	2.653	$p < 0.05$
Costa Nova	1.848	0.829	2.229	$p < 0.05$
Peniche	2.865	1.039	2.757	$p < 0.05$
Cascais	5.669	0.797	7.117	$p < 0.05$
Galapos	2.983	0.526	5.667	$p < 0.05$
Sines	7.792	1.753	4.445	$p < 0.05$
Zavial	2.612	0.915	2.855	$p < 0.05$

When looking at the relative fecundity values, larger RF values were reached in 2017 in comparison to 2014, but also a different spatial pattern was observed between years (Figure 4; Table 2). During 2014, RF values were low at the north and central coast locations and increased almost exponentially towards the southernmost populations (Galapos, Sines and Zavial). Conversely, during 2017, RF increased linearly from the northernmost location to the central coast, reaching a maximum at Cascais which was followed by a sharp drop in RF towards the southernmost locations (Figure 4).

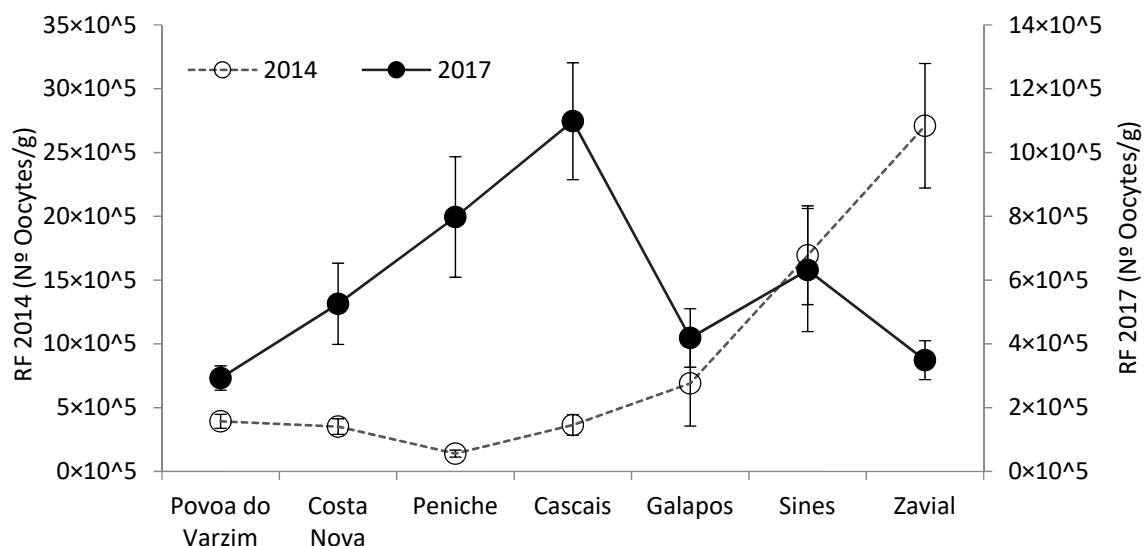


Figure 4. Average and standard error of relative fecundity (RF, n°. oocytes per gram of gonad) in the different locations along the Portuguese coastline, from North (left) to South (right), during the years of 2014 and 2017.

According to the AIC, the four variables used to assess the effect of long-term ($T > 14^\circ\text{C}$ and Max. Chl-a) and short-term (Average SST and Average Chl-a) environmental variability on RF were included in the GAM, explaining 26.6% of the variability

observed across years and locations (Tables 5 and 6; Figure 5). Despite max. Chl-a not showing a significant effect on RF, the variable was maintained in the model because of its traction over AIC (Tables 5 and 6; Figure 5D). The number of days with temperatures over 14 °C during the previous 4 months was the variable with the larger influence on RF (lowest *p*-value; Table 6). The highest positive effect of T > 14 °C was around 80 days, with a sharp detrimental effect on RF when warm days overpassed 100 days (Figure 5A). Average SST and Average Chl-a during the previous month had a similar influence on RF (*p*-values; Table 6), but while Average Chl-a showed a positive and linear relationship with RF (Figure 5C), Average SST only seemed to exert an effect when temperatures rose above 16 °C (Figure 5B).

Table 5. Summary of Akaike Information Criteria (AIC) for the selection of optimal set of variables for inclusion in the model to explaining relative fecundity (RF) along the Portuguese coastline during 2014 and 2017 (grouped years). Short-term variables: average Sea Surface Temperature (Av. SST, °C) and Average Chlorophyll-a concentration (Av. Chl-a, mg/m³), both at last month before the sampling. Long-term variable: number of days with Sea Surface Temperature over 14 °C (T > 14 °C) during the 4 months before the sampling date and Average Chl-a concentration during 10 days around the peak of the spring transition (Max. Chl-a). Variables values used for the analysis were average for each location and year (d.f.: estimated degrees of freedom).

Model	df	AIC
Av. SST	3.000	403.786
AV. Chl-a	4.799	329.071
Days T > 14 °C	4.947	370.316
Max. Chl-a	3.000	353.635
Av. SST + Av. Chl-a	6.656	283.465
Av. SST + Days T > 14 °C	5.840	330.819
Av. SST + Max Chl-a	6.700	329.336
Av. Chl-a + Days T > 14 °C	7.042	286.272
Av. Chl-a + Max. Chl-a	7.940	296.542
Max. Chl-a + Days T > 14 °C	4.950	370.316
Av. SST + Av. Chl-a + Days T > 14 °C	7.460	284.044
Av. SST + Av. Chl-a + Max. Chl-a	9.883	278.559
Days T > 14 °C + Av. Chl-a + Max. Chl-a	10.789	278.181
Av. SST+ Days T > 14 °C + Av. Chl-a + Max. Chl-a	9.943	277.323

Table 6. Structure of the General Additive Model describing the best subset of environmental variables explaining relative fecundity (RF) along the Portuguese coastline from 2014 and 2017, grouped. Averages of Chlorophyll-a (Av. Chl-a, mg/m³) and Sea Surface Temperature (Av. SST, °C) at last month before samples. Number of days with Sea Surface Temperature higher than 14 °C at last 4 months (N Days SST > 14 °C). Average Chl-a concentration during 10 days around the peak of the spring transition (Max. Chl-a). S.E.: standard error; e.d.f.: estimated degrees of freedom.

	Parametric Coefficients			
	Estimate	S.E.	T	<i>p</i>
Intercept	5.494	0.028	198.300	< 2 × 10 ⁻¹⁶
Smooth terms (non parametric)				
	e.d.f	F	<i>p</i>	
N Days T > 14 °C	3.0	8.277	2.9 × 10 ⁻⁵	
Av. SST	2.4	7.150	0.0018	
Av. Chl-a	1.0	8.105	0.0048	
Max. Chl-a	1.6	0.530	0.4880	
R ² adjusted: 0.241		% Deviance explained: 26.6%		

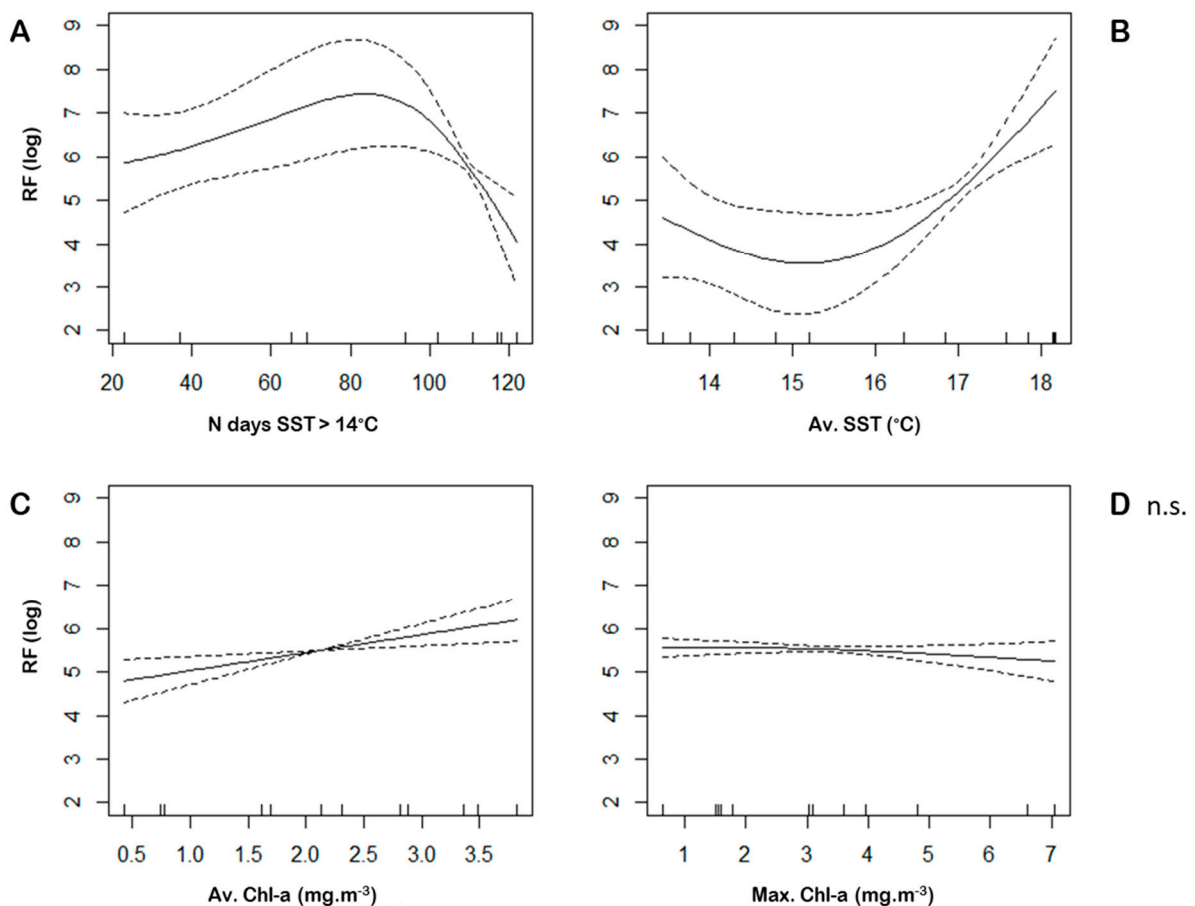


Figure 5. Results of the General Additive Model showing the best subset of environmental variables explaining relative fecundity (RF, log) along the Portuguese coastline, during 2014 and 2017 (grouped years). (A) Number of days with Sea Surface Temperature higher than 14 °C at last 4 months (N Days SST > 14 °C). (B) Average of Sea Surface Temperature (Av. SST, °C) and (C) Chlorophyll-a (Av. Chl-a, mg/m³) at last month before samples. (D) Chl-a concentration during 10 days around the peak of the spring transition (max. Chl-a). Dashed lines show 95% Confidence Interval and tick marks along the x-axis represent where the RF values (points) occurred.

4. Discussion

Temperature latitudinal gradients are usually explored to understand the effects of thermal stress on marine invertebrates and to try to predict the subsequent impacts of future climate change scenarios over their distribution and population dynamics [21,40–42]. Our study explores the reproductive output of mussel populations along a latitudinal gradient at the North Atlantic south limit of *Mytilus galloprovincialis* distribution. The sampled populations cover a temperature range of 1.5 °C from the northernmost to the southernmost locations (Table 1) which encompass the predicted rise of SST by 2100 under certain climate change scenarios (1.2 to 3.6 °C for RCP2.6 and RCP8.5 respectively) [1]. The temperature latitudinal gradient observed in our study area goes along with a trend of rising salinity and decreasing Chl-a availability from North to South (Table 1). Nonetheless, while the temperature differences between extreme locations was stable between years (1.5 °C even when average temperature was much larger in 2017 than in 2014), for salinity and Chl-a, spatial variability was not so consistent (Table 1). Maximum Chl-a and minimum salinity values were detected at the northernmost location in both years, even if lower riverine inputs and a much larger phytoplankton bloom during spring transition occurred in 2014 (Figure 2), but the progressive trend towards the south was not monotonic (Table 1). Other local factors like riverine inputs, upwelling intensity or topography may have a larger influence over the spatio-temporal variability of those variables, preventing in many cases a direct correlation of Chl-a and salinity with latitude [21].

The large spatio-temporal variability on relevant environmental variables (food availability, wave intensity, air exposure, topographical characteristics, etc.) coupled to complex interactions and trade-offs between them and temperature, has been frequently suggested as an explanation for the lack of detection of latitudinal gradients on physiological performance attributable to an increase of thermal stress [21,40–42]. Particularly, for mussel reproductive output, the lack of detection of a thermal stress latitudinal gradient is commonly attributed to the large influence of food availability on the reproductive processes [7,20,23]. Food availability regulates the number of oocytes produced [25], but also modulates stress response capability and metabolic activity in mussels, increasing their ability to cope with different sources of stress [43]. Some authors identify more complex interactions between environmental variables, but associated to oceanographic processes which lead to the persistence of multivariate mosaics of optimal environmental conditions and therefore maximum reproductive investment [21].

Our results showed that 3 locations in the Central-North coast of Portugal (Peniche, Cascais and Costa Nova) registered the largest absolute fecundity values during both years (Figure 3A). Egg production per individual was much higher in 2017 than in 2014, suggesting a larger influence of temperature over food availability for the reproductive output of those populations, since 2017 was characterized by warmer temperatures and lower food availability (Table 1; Figure 2). Nonetheless, the higher values observed for AF at those locations, both during 2014 and 2017, seems to be driven by the larger size of mussels at these three populations (Figure 3B). Mussels, as well as many iteroparous invertebrates, show a direct relationship between reproductive effort and body size, which is usually explained as an age-related increase on the proportion of energy allocated to reproduction [24,25,44,45]. Our results highlight the relationship between size and AF for all the populations and years studied (Table 3). Nonetheless, slopes describing the relationship between AF and size varied between locations (Figure 3C), which might be a consequence of the amount of stress experienced at each population. Previous studies have suggested that environmental stress can push populations of mussels to reach reproductive maturity at smaller sizes [46,47], as well as to attain earlier their maximum rate of reproductive investment, resulting in steeper slopes between reproductive effort and size [44]. Optimal environmental conditions usually lead to less stressed and faster growing populations, which reach reproductive maturity at larger sizes but also attain larger life spans [44–47]. Several authors have reported a decay on reproductive output on mussels over 50 mm, related to senescence processes [37,44,48], which can also flatten the slope of the relationship between oocyte production and size in populations where average size was larger (Figure 3). A combination of both processes might determine the relationship of reproductive output with size at each population [44], and agree with the hypothesis of persistent multivariate mosaics of environmental conditions which determine the adaptation of each population to their local habitat [21], and comply with the consistence of the slopes calculated for each location between years in the present study (Table 4; Figure 3C).

The standardization of AF by gonad weight (RF) allows for the integration of size on the reproductive output of each population, and for the detection of further latitudinal patterns which vary between years (Figure 4). In 2014, RF increased almost exponentially towards the south, suggesting almost a linear effect of temperature on reproductive output over certain thresholds (Table 1; Figure 2). Nonetheless, in 2017 maximum RF values were displaced towards the central coast of Portugal, with a sharp drop of RF farther South (Figure 4), which seems to indicate that the warmer temperatures detected that year (Table 1; Figure 2) overpassed reproductive optimums at those locations, even when temperatures recorded were far from the upper thermal limit reported for the species ($\approx 27\text{--}35^\circ\text{C}$; [7,28]).

Gonadal development of mussels and many other bivalves takes place over a range of temperatures which are usually well below their thermal tolerance limit for survival [34,49–51]. Temperature influences metabolic rates, increasing energetic cost and limiting the energy

available for reproduction [24]. For *M. galloprovincialis*, energy allocation for reproduction seems to decrease fast when temperature rises over the optimum for somatic maintenance (≈ 17.5 °C; [28]), leading to a reproduction limiting temperature around 19 °C [34]. RF latitudinal gradients observed in the present study (Figure 4) might reflect the thermal history of mussels during gametogenesis according to those limits, reaching maximum values at those locations and years where temperature (Figure 2) was between the reported optimum (≈ 14 °C; [34]) for *M. galloprovincialis* gamete production and its upper limit (19 °C; [34]). Food availability can compensate for the extra demand of energy under certain stress conditions [43], but several studies report decreased rates of gametogenesis under high temperatures for bivalves, even under no limiting food conditions [34,50,51].

Our GAM model also reflects a larger effect of the temperature history over the food availability on gamete production (Table 6), supporting the role of temperature as a switching-on/-off mechanism for gametogenesis (Figure 5A). The number of days with temperatures over the optimum for gamete production during gametogenesis (4 months) explained the largest amount of the variability observed on RF (p -value $< 2.9 \times 10^{-5}$; Table 6). RF increases slightly with the number of warm days until those overpasses certain limit (≈ 80 days; Figure 5A) leading to a sharp drop on reproductive output. "Temperature windows" for gametogenesis are well documented for bivalves [25] and their evolution is usually associated with the advantage of matching reproduction with optimal conditions for larval development [52]. For *M. galloprovincialis* in the Iberian Coast, two peaks of reproduction are commonly reported (spring and autumn) [36,53], when food availability and oceanographic conditions optimize larval survival [52,54]. Therefore, having temperature thresholds for gametogenesis to avoid energy allocation for gamete production during winter and summer, when larval survival is limited by environmental conditions, might be a good strategy for energy optimization.

It is well known that temperature has multiple effects over bivalves' gametogenesis, first acting as an on/off mechanism, and once activated regulating its kinetics [55]. Our results also highlighted a positive effect of temperature over RF when it rises over 16 °C during the last month of gametogenesis (Figure 5B). The average temperature values recorded during our study did not reach the reproduction limiting temperature (19 °C [34]) at any time (Figure 5B). Therefore, the positive relationship observed between temperature and RF during the last month of gametogenesis is not expected to be maintained over that temperature threshold.

We also detected a linear and positive effect of Chl-a concentration during the last month of gametogenesis over RF (Figure 5C), while the maximum Chl-a attained during the spring bloom had no significant effect on the reproductive output (Figure 5D; Table 6). These results might indicate that mussels are taking an opportunistic reproductive strategy, since the reproductive output is only dependent of the most recent food concentration. Food availability has a direct effect over the amount and quality of gametes produced by bivalves, but according to their reproductive strategy, species can be classified as opportunistic or conservative [24,56]. In opportunistic species the gametogenesis is linked to the food supply and occurs when feeding conditions are favourable, while in the conservative species the nutrients are stored before gametogenesis is initiated [24]. Mussels are, however, quite flexible and can exhibit both types of strategy, adapting it to the prevailing environmental conditions [24]. For some authors, gametogenesis initiation is mostly limited by nutrient availability, either as reserves or recently ingested food [45], while for others it is the temperature window which determines initiation/cessation of gametogenesis, and food availability modulates the amount of gametes produced [24]. Our results support better the second hypothesis, since we detected a much lower influence of food availability than temperature over RF (Table 6). The patterns observed (Figure 5) also agree with a major role of accumulative temperature conditions acting as a switching-on/off mechanism for gametogenesis, while more recent environmental conditions (temperature and food availability) regulate gamete production rates.

IPPC predicted a rise of SST by 2100 ranges from 1.2 to 3.6 °C (for RCP2.6 and RCP8.5 respectively; [1]). Our results suggest that under these climate predictions, temperature windows for gametogenesis will limit the number of reproductive events and might also alter the reproductive phenology of mussels to avoid persistent warm temperatures which will start earlier in the year and last for longer. Many studies agree on predicting changes on reproductive phenology of mussels [7,9,28,52], because an earlier activation of gametogenesis but an upper temperature limit controlling the decline of gametogenesis is not commonly included. Therefore, even when mismatch effects of dislodging reproduction towards less favourable conditions for larval survival might negatively affect mussel population dynamics [52,53], many studies based on DEB models consistently predict a maintenance or a slight increase of reproductive output for bivalves, and an increase of the population performance in all the locations where warming future scenarios don't overpass thermal lethal tolerance of the species [7,9,20,23,27–30]. As mentioned before, those results might be related to the lack of specific parametrization of non-linear responses of gamete production to environmental conditions. DEB models establish general rules and priorities for energy allocation (somatic maintenance > growth > maturity maintenance > reproduction), and estimations of the cost of different physiological processes [31]. In addition, DEB models establish a series of assumptions for bivalve reproduction which usually include: a threshold of degree-days to activate gametogenesis, a threshold of gonadosomatic index to achieve ripe condition and a temperature threshold to trigger spawning [7,9,20,23,27–30]. However, those models do not include an upper limit for gametogenesis [9,20,23,27–30]. With the exception of some studies which incorporate a thermal upper limit for spawning [7], the lack of a specific upper limit for gametogenesis and the assumption that reproduction follows the same thermal tolerance rules than other physiological processes [31] forces the predictions towards large reproductive outputs [9,20,23,27–30], even at temperatures over the reported limit for reproduction [34]. The lack of correct parameterization of gametogenesis can therefore overestimate mussel population performance under future climate change scenarios.

Our results deepen the understanding of the underlying processes controlling the complex interactions between environmental drivers and gamete production, particularly highlighting the relevance of considering the thermal window for gametogenesis. Our study also points out the relevance of a correct parameterization of those processes, to be able to perform accurate predictions of population performance under future climate change scenarios.

5. Conclusions

Our study supports the view that gametogenesis responds non-linearly to temperature and chlorophyll concentrations, and that these variables show different effects over fecundity depending on the temporal scale evaluated. We found a major role of long-term temperature, acting as a switching on-off mechanism for gametogenesis, while short-term food availability has a lower influence but also modulates the amount of gametes produced.

Our results highlight the complexity of gametogenesis environmental dependences, and how its inclusion in predictive models is vital to avoid overestimations on the capability of mussel populations to deal with climate change future scenarios.

Author Contributions: Conceptualization, H.Q. and L.G.P.; methodology, G.F.O., H.S., H.Q., L.G.P.; formal analysis, G.F.O., H.S., H.Q. and L.G.P.; investigation, G.F.O., H.S., H.Q. and L.G.P.; resources, H.Q.; data curation, G.F.O., H.S., H.Q. and L.G.P.; writing—original draft preparation, G.F.O. and L.G.P.; writing—review and editing, G.F.O., H.Q. and L.G.P.; supervision, H.Q. and L.G.P.; funding acquisition, G.F.O., H.Q. and L.G.P. All authors have read and agreed to the published version of the manuscript.

Funding: This study is part of the 'Larval Sources-Assessing the ecological performance of marine protected area networks' research project, funded by Fundação para a Ciência e Tecnologia-FCT/MCTES (PTDC/BIA-BIC/120483/2010). Financial support was allocated under the COMPETE Programme, which includes components from the European Regional Development Fund and from

the Ministério da Ciência, Tecnologia e Ensino Superior. Thanks are also due to FCT/MCTES for the financial support to CESAM (UIDP/50017/2020+UIDB/50017/2020), through national funds. G.F.O. was supported by a grant from Coordenação de Aperfeiçoamento de Pessoal de Nível Superior–Brasil (CAPES)–Finance Code 001, grant number 13724/13-4 L.G.P. was supported by a postdoctoral fellowship from Xunta de Galicia, Spain (POS-B/2016/032) during the field work and by a Talento Senior Grant (16_IN585A_2020_986937) during the writing of the manuscript. H.S. was supported by a grant from the Erasmus Mundus Master of Science in Marine Biodiversity and Conservation.

Institutional Review Board Statement: Ethical review and approval were waived for this study because this is a very abundant and non-endangered species. Samples taken were only those strictly necessary for the analyses, and were made under permission of the Agência Portuguesa do Ambiente and the Instituto de Conservação da Biodiversidade e Florestas.

Informed Consent Statement: Not applicable.

Data Availability Statement: The datasets generated and analyzed during this study are available from the corresponding author upon request.

Acknowledgments: The authors would like to thank Inês Gomes, Rui Albuquerque and Rafael Batista (Universidade de Aveiro), as well as Cláudia Moreira and Ana Margarida Gama (Centro Interdisciplinar de Investigação Marinha e Ambiental, Universidade do Porto) and João Castro (Laboratório de Ciências do Mar da Universidade de Évora) for their support during the fieldwork and laboratory analysis. We also would like to thank Maria de Jesus Fernandes, Director of the Departamento de Conservação da Natureza e Florestas de Lisboa e Vale do Tejo of the Instituto de Conservação da Natureza e Florestas, who issued sampling permits and provided access to facilities of the Reserva Natural das Berlengas (RNB) and the Parque Natural da Arrábida (PNA). Licenses for rocky shore sampling outside the protected areas were provided by the Agência Nacional do Ambiente.

Conflicts of Interest: The authors declare no conflict of interest. The funders had no role in the design of the study; in the collection, analyses, or interpretation of data; in the writing of the manuscript, or in the decision to publish the results.

References

1. Bindoff, N.L.; Cheung, W.W.L.; Kairo, J.G.; Aristegui, J.; Guinder, V.A.; Hallberg, R.; Hilmi, N.; Jiao, N.; O'Donoghue, S.; Suga, T.; et al. Changing Ocean, Marine Ecosystems, and Dependent Communities. In *IPCC Special Report on the Ocean and Cryosphere in a Changing Climate*; Intergovernmental Panel on Climate Change: Geneva, Switzerland, 2019; pp. 477–587.
2. Doney, S.C.; Ruckelshaus, M.; Duffy, J.E.; Barry, J.P.; Chan, F.; English, C.A.; Galindo, H.M.; Grebmeier, J.; Hollowed, A.B.; Knowlton, N.; et al. Climate Change Impacts on Marine Ecosystems. *Annu. Rev. Mar. Sci.* **2012**, *4*, 11–37. [[CrossRef](#)]
3. Gattuso, J.-P.; Magnan, A.K.; Billé, R.; Cheung, W.W.L.; Howes, E.L.; Joos, F.; Allemand, D.; Bopp, L.; Cooley, S.R.; Eakin, C.M.; et al. Contrasting futures for ocean and society from different anthropogenic CO₂ emissions scenarios. *Science* **2015**, *349*, aac4722. [[CrossRef](#)]
4. Hoegh-Guldberg, O.; Bruno, J.F. The Impact of Climate Change on the World's Marine Ecosystems. *Science* **2010**, *328*, 1523–1528. [[CrossRef](#)]
5. Scheffers, B.R.; De Meester, L.; Bridge, T.C.L.; Hoffmann, A.; Pandolfi, J.; Corlett, R.; Butchart, S.H.M.; Pearce-Kelly, P.; Kovacs, K.M.; Dudgeon, D.; et al. The broad footprint of climate change from genes to biomes to people. *Science* **2016**, *354*, aaf7671. [[CrossRef](#)]
6. Santos, C.F.; Agardy, T.; Andrade, F.; Calado, H.; Crowder, L.B.; Ehler, C.N.; García-Morales, S.; Gissi, E.; Halpern, B.S.; Orbach, M.K.; et al. Integrating climate change in ocean planning. *Nat. Sustain.* **2020**, *3*, 505–516. [[CrossRef](#)]
7. Thomas, Y.; Bacher, C. Assessing the sensitivity of bivalve populations to global warming using an individual-based modelling approach. *Glob. Chang. Biol.* **2018**, *24*, 4581–4597. [[CrossRef](#)] [[PubMed](#)]
8. Froehlich, H.E.; Gentry, R.R.; Halpern, B.S. Global change in marine aquaculture production potential under climate change. *Nat. Ecol. Evol.* **2018**, *2*, 1745–1750. [[CrossRef](#)] [[PubMed](#)]
9. Steeves, L.E.; Filgueira, R.; Guyondet, T.; Chassé, J.; Comeau, L. Past, Present, and Future: Performance of Two Bivalve Species Under Changing Environmental Conditions. *Front. Mar. Sci.* **2018**, *5*, 184. [[CrossRef](#)]
10. Hare, J.A.; Morrison, W.E.; Nelson, M.W.; Stachura, M.M.; Teeters, E.J.; Griffis, R.; Alexander, M.; Scott, J.D.; Alade, L.; Bell, R.J.; et al. A Vulnerability Assessment of Fish and Invertebrates to Climate Change on the Northeast U.S. Continental Shelf. *PLoS ONE* **2016**, *11*, e0146756. [[CrossRef](#)] [[PubMed](#)]
11. Smith, J.R.; Fong, P.; Ambrose, R.F. Dramatic declines in mussel bed community diversity: Response to climate change? *Ecology* **2006**, *87*, 1153–1161. [[CrossRef](#)]

12. Froján, M.; Figueiras, F.G.; Zúñiga, D.; Pérez, F.A.; Arbones, B.; Castro, C.G. Influence of Mussel Culture on the Vertical Export of Phytoplankton Carbon in a Coastal Upwelling Embayment (Ría de Vigo, NW Iberia). *Estuaries Coasts* **2016**, *39*, 1449–1462. [[CrossRef](#)]
13. Petersen, J.K.; Saurel, C.; Nielsen, P.; Timmermann, K. The use of shellfish for eutrophication control. *Aquac. Int.* **2015**, *24*, 857–878. [[CrossRef](#)]
14. Food and Agriculture Organization (FAO). *The State of World Fisheries and Aquaculture 2020: Sustainability in Action*; The State of World Fisheries and Aquaculture (SOFIA); Food and Agriculture Organization: Rome, Italy, 2020.
15. Science Advice for Policy by European Academies. *Food from the Oceans: How Can More Food and Biomass Be Obtained from the Oceans in a Way That Does Not Deprive Future Generations of Their Benefits*; SAPEA: Berlin, Germany, 2017.
16. Farcy, É.; Burgeot, T.; Haberkorn, H.; Auffret, M.; Lagadic, L.; Allenou, J.-P.; Budzinski, H.; Mazzella, N.; Pete, R.; Heydorff, M.; et al. An integrated environmental approach to investigate biomarker fluctuations in the blue mussel *Mytilus edulis* L. in the Vilaine estuary, France. *Environ. Sci. Pollut. Res.* **2012**, *20*, 630–650. [[CrossRef](#)] [[PubMed](#)]
17. Fly, E.K.; Hilbish, T.J.; Wethey, D.; Rognstad, R.L. Physiology and Biogeography: The Response of European Mussels (*Mytilus* spp.) to Climate Change. *Am. Malacol. Bull.* **2015**, *33*, 136–149. [[CrossRef](#)]
18. Kroeker, K.J.; Gaylord, B.; Hill, T.M.; Hosfelt, J.D.; Miller, S.H.; Sanford, E. The Role of Temperature in Determining Species' Vulnerability to Ocean Acidification: A Case Study Using *Mytilus galloprovincialis*. *PLoS ONE* **2014**, *9*, e100353. [[CrossRef](#)] [[PubMed](#)]
19. Zippay, M.L.; Helmuth, B. Effects of temperature change on mussel, *Mytilus*. *Integr. Zool.* **2012**, *7*, 312–327. [[CrossRef](#)]
20. Gourault, M.; Petton, S.; Thomas, Y.; Pecquerie, L.; Marques, G.; Cassou, C.; Fleury, E.; Paulet, Y.-M.; Pouvreau, S. Modeling reproductive traits of an invasive bivalve species under contrasting climate scenarios from 1960 to 2100. *J. Sea Res.* **2019**, *143*, 128–139. [[CrossRef](#)]
21. McCabe, M.; Navarrete, S. Reproductive investment in rocky intertidal mussels: Spatiotemporal variability and environmental determinants. *Mar. Ecol. Prog. Ser.* **2018**, *599*, 107–124. [[CrossRef](#)]
22. Gosling, E. Reproduction, Settlement and Recruitment. In *Bivalve Molluscs: Biology, Ecology and Culture*; Fishing News Books: Oxford, UK, 2003; pp. 131–168.
23. Bernard, I.; de Kermoisan, G.; Pouvreau, S. Effect of phytoplankton and temperature on the reproduction of the Pacific oyster *Crassostrea gigas*: Investigation through DEB theory. *J. Sea Res.* **2011**, *66*, 349–360. [[CrossRef](#)]
24. Seed, R.; Suchanek, T. Population and community ecology of *Mytilus*. In *The Mussel Mytilus: Ecology, Physiology, Genetics and Culture*; Gosling, E., Ed.; Elsevier: San Diego, CA, USA, 1992; pp. 87–170.
25. Gosling, E. (Ed.) Reproduction, Settlement and Recruitment. In *Marine Bivalve Molluscs*; John Wiley & Sons: Oxford, UK, 2015; pp. 157–202.
26. Starr, M.; Himmelman, J.H.; Therriault, J.-C. Direct Coupling of Marine Invertebrate Spawning with Phytoplankton Blooms. *Science* **1990**, *247*, 1071–1074. [[CrossRef](#)]
27. Monaco, C.J.; McQuaid, C. Climate warming reduces the reproductive advantage of a globally invasive intertidal mussel. *Biol. Invasions* **2019**, *21*, 2503–2516. [[CrossRef](#)]
28. Montalto, V.; Helmuth, B.; Ruti, P.M.; Dell'Aquila, A.; Rinaldi, A.; Sarà, G. A mechanistic approach reveals non linear effects of climate warming on mussels throughout the Mediterranean sea. *Clim. Chang.* **2016**, *139*, 293–306. [[CrossRef](#)]
29. Sara, G.; Palmeri, V.; Rinaldi, A.C.; Montalto, V.; Helmuth, B. Predicting biological invasions in marine habitats through eco-physiological mechanistic models: A case study with the bivalve *Brachidontes pharaonis*. *Divers. Distrib.* **2013**, *19*, 1235–1247. [[CrossRef](#)]
30. Sara, G.; Palmeri, V.; Montalto, V.; Rinaldi, A.; Widdows, J. Parameterisation of bivalve functional traits for mechanistic eco-physiological dynamic energy budget (DEB) models. *Mar. Ecol. Prog. Ser.* **2013**, *480*, 99–117. [[CrossRef](#)]
31. Kooijman, B. *Dynamic Energy Budget Theory for Metabolic Organisation*; Cambridge University Press: Cambridge, UK, 2010.
32. Pörtner, H.-O.; Gutt, J. Impacts of Climate Variability and Change on (Marine) Animals: Physiological Underpinnings and Evolutionary Consequences. *Integr. Comp. Biol.* **2016**, *56*, 31–44. [[CrossRef](#)]
33. Christensen, E.A.F.; Norin, T.; Tabak, I.; van Deurs, M.; Behrens, J.W. Effects of temperature on physiological performance and behavioral thermoregulation in an invasive fish, the round goby. *J. Exp. Biol.* **2021**, *224*, 237669. [[CrossRef](#)]
34. Fearman, J.; Moltschanowskyj, N. Warmer temperatures reduce rates of gametogenesis in temperate mussels, *Mytilus galloprovincialis*. *Aquaculture* **2010**, *305*, 20–25. [[CrossRef](#)]
35. Cáceres-Martínez, J.; Figueras, A. Long-term survey on wild and cultured mussels (*Mytilus galloprovincialis* Lmk) reproductive cycles in the Ria de Vigo (NW Spain). *Aquaculture* **1998**, *162*, 141–156. [[CrossRef](#)]
36. Villalba, A. Gametogenic cycle of cultured mussel, *Mytilus galloprovincialis*, in the bays of Galicia (N.W. Spain). *Aquaculture* **1995**, *130*, 269–277. [[CrossRef](#)]
37. Sukhotin, A.A.; Flyachinskaya, L.P. Aging reduces reproductive success in mussels *Mytilus edulis*. *Mech. Ageing Dev.* **2009**, *130*, 754–761. [[CrossRef](#)] [[PubMed](#)]
38. R Core Team. *R: A Language and Environment for Statistical Computing*; R Foundation for Statistical Computing: Vienna, Austria, 2018.
39. Zuur, A.; Ieno, E.N.; Walker, N.; Saveliev, A.A.; Smith, G.M. *Mixed Effects Models and Extensions in Ecology with R*; Springer: New York, NY, USA, 2009.

40. Helmuth, B.; Harley, C.; Halpin, P.M.; O'Donnell, M.; Hofmann, G.E.; Blanchette, C.A. Climate Change and Latitudinal Patterns of Intertidal Thermal Stress. *Science* **2002**, *298*, 1015–1017. [[CrossRef](#)]
41. Sara', G.; Kearney, M.; Helmuth, B. Combining heat-transfer and energy budget models to predict thermal stress in Mediterranean intertidal mussels. *Chem. Ecol.* **2011**, *27*, 135–145. [[CrossRef](#)]
42. Newell, R.I.E.; Hilbish, T.J.; Koehn, R.K.; Newell, C.J. Temporal Variation in the Reproductive Cycle of *Mytilus edulis*. (Bivalvia, Mytilidae) from Localities on the East Coast of the United States. *Biol. Bull.* **1982**, *162*, 299–310. [[CrossRef](#)]
43. Dowd, W.W.; Felton, C.A.; Heymann, H.M.; Kost, L.E.; Somero, G.N. Food availability, more than body temperature, drives correlated shifts in ATP-generating and antioxidant enzyme capacities in a population of intertidal mussels (*Mytilus californianus*). *J. Exp. Mar. Biol. Ecol.* **2013**, *449*, 171–185. [[CrossRef](#)]
44. Bayne, B.L.; Salkeld, P.N.; Worrall, C.M. Reproductive effort and value in different populations of the marine mussel, *Mytilus edulis* L. *Oecologia* **1983**, *59*, 18–26. [[CrossRef](#)]
45. Bayne, B.; Worrall, C. Growth and Production of Mussels *Mytilus edulis* from Two Populations. *Mar. Ecol. Prog. Ser.* **1980**, *3*, 317–328. [[CrossRef](#)]
46. Sprung, M. Reproduction and fecundity of the mussel *Mytilus edulis* at helgoland (North sea). *Helgol. Mar. Res.* **1983**, *36*, 243–255. [[CrossRef](#)]
47. Seed, R. The ecology of *Mytilus edulis* L. (Lamellibranchiata) on exposed rocky shores. *Oecologia* **1969**, *3*, 277–316. [[CrossRef](#)] [[PubMed](#)]
48. Rodhouse, P.; McDonald, J.H.; Newell, R.I.E.; Koehn, R.K. Gamete production, somatic growth and multiple-locus enzyme heterozygosity in *Mytilus edulis*. *Mar. Biol.* **1986**, *90*, 209–214. [[CrossRef](#)]
49. Beukema, J.J.; Dekker, R.; Jansen, J.M. Some like it cold: Populations of the tellinid bivalve *Macoma balthica* (L.) suffer in various ways from a warming climate. *Mar. Ecol. Prog. Ser.* **2009**, *384*, 135–145. [[CrossRef](#)]
50. Heasman, M.; O'Connor, W.; Frazer, A. Temperature and nutrition as factors in conditioning broodstock of the commercial scallop *Pecten fumatus* Reeve. *Aquaculture* **1996**, *143*, 75–90. [[CrossRef](#)]
51. Martínez, G.; Pérez, H. Effect of different temperature regimes on reproductive conditioning in the scallop *Argopecten purpuratus*. *Aquaculture* **2003**, *228*, 153–167. [[CrossRef](#)]
52. Philippart, C.J.M.; Van Bleijswijk, J.D.L.; Kromkamp, J.C.; Zuur, A.F.; Herman, P. Reproductive phenology of coastal marine bivalves in a seasonal environment. *J. Plankton Res.* **2014**, *36*, 1512–1527. [[CrossRef](#)]
53. Philippart, C.J.; Amaral, A.; Asmus, R.; Van Bleijswijk, J.; Bremner, J.; Buchholz, F.; Cabanellas-Reboredo, M.; Catarino, D.; Cattrijsse, A.; Charles, F.; et al. Spatial synchronies in the seasonal occurrence of larvae of oysters (*Crassostrea gigas*) and mussels (*Mytilus edulis/galloprovincialis*) in European coastal waters. *Estuar. Coast. Shelf Sci.* **2012**, *108*, 52–63. [[CrossRef](#)]
54. Peteiro, L.G.; Labarta, U.; Fernández-Reiriz, M.; Alvarez-Salgado, X.; Filgueira, R.; Piedracoba, S. Influence of intermittent-upwelling on *Mytilus galloprovincialis* settlement patterns in the Ría de Ares-Betanzos. *Mar. Ecol. Prog. Ser.* **2011**, *443*, 111–127. [[CrossRef](#)]
55. Navarro, E.; Iglesias, J.I.P. Energetics of reproduction related to environmental variability in bivalve molluscs. *Haliotis* **1995**, *24*, 43–55.
56. Bayne, B.L. Aspects of reproduction in bivalve molluscs. In *Estuarine Processes*; Wiley, M., Ed.; Academic Press: New York, NY, USA, 1976; pp. 432–448.